ISSN 1069-3513, Izvestiya, Physics of the Solid Earth, 2010, Vol. 46, No. 7, pp. 602–612. © Pleiades Publishing, Ltd., 2010.
Original Russian Text © M.Yu. Reshetnyak, 2010, published in Fizika Zemli, 2010, No. 7, pp. 52–63.

Nonlinearities in Dynamo

M. Yu. Reshetnyak

Schmidt Institute of Physics of the Earth, Russian Academy of Sciences,
ul. Bol'shaya Gruzinskaya 10, Moscow, 123995 Russia
E-mail: m.reshetnyak@graail.com

Received November 3, 2009

Abstract—By the example of the dynamo model in the rotating plane layer heated from below, the effects are examined that lead to the stabilization of an exponentially growing magnetic field in the magnetostrophic convection in passing from the kinematic dynamo mode to the nonlinear mode. The estimates of the energy redistribution in the spectrum are given, and the mechanisms of suppression of helicity are presented. Equalization of the field of velocity and the magnetic field is analyzed. The modes examined are close to those utilized in the up-to-date models of the planetary dynamo in the cores of planets.

Key words: liquid core, heat convection, dynamo, helicity.

DOI: 10.1134/S1069351310070049

1. INTRODUCTION

Many physical processes can be attributed to the threshold phenomena, when an increase in a certain parameter leads to the appearance of a growing solution. An example of such processes is heat convection, when an increase in the amplitude of thermal sources results in the appearance of an exponentially growing solution for temperature T and velocity $\mathbf{V}$. The growth begins at a certain critical value of the Rayleigh number Ra^{cr} that characterizes the amplitude of the thermal sources [Chandrasekhar, 1961]. A similar situation is also observed for the generation of the magnetic field $\mathbf{B}$ in a conductive medium: by increasing the intensity of the convective sources (i.e., by increasing the magnetic Reynolds number up to $\mathrm{R}_\mathrm{m}^{cr}$), it is possible to obtain an exponentially growing solution for a number of flows [Moffat, 1978]. The magnetic field further increases until it begins influencing the flow. It turns out that such influence is not reduced to the direct suppression of motion and to the decrease of the Reynolds number, but more probably leads to the rearrangement of flows in order that to provide a less effective generation of the field. The intensity of the flows itself sometimes can even increase at the passage from nonmagnetic convection to a magnetic one and, in any case, the magnetic Reynolds number may be several orders of magnitude larger than $\mathrm{R}_\mathrm{m}^{cr}$, as this occurs in astrophysical objects, providing the sufficiently long spectra of the magnetic field. This means that the information concerning the value of R_m is insufficient to answer the question on whether the magnetic field will further increase or not.

On the other hand, the visual analysis of flows in passing from the nonmagnetic state to the magnetic one does not yield a clear answer to the question, concerning the reason for the retardation of an increase in the magnetic field and the passage of the system into a quasi-stationary state. In other words, the magnetic field only faintly affects even the qualitative structure of the flow [Jones, 2000], which indicates the preference of the magnetic field to the force-free configurations ($|(\nabla \times \mathbf{B}) \times \mathbf{B}|\, \mathrm{L}_\mathrm{B}/B^2 \ll 1$, where L_B is the energy-bearing scale of the magnetic field). Recently, a number of works appeared (see review in [Brandenburg and Subramanian, 2005]) where the effects, associated with the redistribution of energy over the spectrum and with the appearance of the different-scale helicities in the magnetic field, are noted as the mechanisms of stabilization. Below, we see how such a redistribution of magnetic energy is also observed in the rotating medium, and also, by the example of 3D calculations of the dynamo in a plane layer, we consider how the appearance of the magnetic helicity results in the suppression of the α effect.

Another important issue in estimating the influence of the magnetic field on the flow is the correlation between the velocity field and the magnetic field (the so-called cross-helicity). It turns out that if we take the velocity field (nonstationary) from the solution of the dynamo problem, when the solution has already passed into the quasi-stationary state, and substitute it in the equation of induction, after solving the problem of the kinematic dynamo for the magnetic field with somewhat disturbed initial conditions (for $\mathbf{B}$), then the magnetic field will begin increasing exponentially in the convective periods [Cattaneo and Tobias, 2009]. Below, we examine this example in more detail in connection with the modes applied in the geodynamo models.

2. THE DYNAMO EQUATIONS

Now, we consider the dynamo equations for an incompressible liquid ($\nabla \cdot \mathbf{V} = 0$) in the infinite layer $0 \le z \le 1$, rotating with an angular velocity Ω relative to the vertical axis z. We introduce the following units of measurement for the velocity $\mathbf{V}$, the time t, the pressure P, and the magnetic field $\mathbf{B}$: κ/L, L^2/κ, $\rho\kappa^2/L^2$ and $\sqrt{2\Omega\rho\kappa\mu_0}$, where L is the unit of length, κ is the coefficient of molecular thermal conductivity, ρ is the density, and μ_0 is the magnetic constant. Then, we can write down the system of dynamo equations in the Cartesian coordinates (x, y, z) in the form (see details in [Reshetnyak, 2007]):

$$\begin{aligned} \frac{\partial \mathbf{B}}{\partial t} &= \operatorname{curl}(\mathbf{V} \times \mathbf{B}) + q^{-1}\Delta\mathbf{B} \\ E\mathrm{Pr}^{-1}\left[\frac{\partial \mathbf{V}}{\partial t} - \mathbf{V} \times (\nabla \times \mathbf{V})\right] &= \operatorname{curl}\mathbf{B} \times \mathbf{B} \\ -\nabla P - 1_z \times \mathbf{V} + \mathrm{Ra}\,T1_z + E\Delta\mathbf{V} & \\ \frac{\partial T}{\partial t} + (\mathbf{V} \cdot \nabla)(T + T_0) &= \Delta T. \end{aligned} \tag{1}$$

The dimensionless Prandtl, Ekman, Rayleigh, and Roberts numbers are specified in the form: $\mathrm{Pr} = \frac{\nu}{\kappa}$, $E = \frac{\nu}{2\Omega L^2}$, $\mathrm{Ra} = \frac{ag_0\delta T L}{2\Omega\kappa}$, and $q = \frac{\kappa}{\eta}$, where ν is the coefficient of the kinematic viscosity, α is the coefficient of volume expansion, g_0 is the gravity acceleration, δT is the unit of the disturbance in temperature T relative to the "diffusion" (nonconvective) temperature distribution $T_0 = 1 - z$, and η is the coefficient of magnetic diffusion. We introduce the Rossby number as $\mathrm{Ro} = E\mathrm{Pr}^{-1}$.

System (1) is closed by the horizontal periodic boundary conditions. For the boundaries $z = 0, 1$, the zero temperature disturbances $T = 0$ are used, which, taking into account the selected profile of T_0, is equivalent to specifying the temperatures on the boundaries: $\mathrm{T} = T + T_0 = 1, 0$. For the field velocity, we assume the condition of nonpenetration and zero gradients of the tangential components on the boundaries $z = 0, 1$: $V_z = \frac{\partial V_x}{\partial z} = \frac{\partial V_y}{\partial z} = 0$. For the magnetic field, the pseudovacuum boundary conditions are used: $B_x = B_y = \frac{\partial B_z}{\partial z} = 0$. The details of the pseudospectral code and the implementation of the program on the multiprocessor computational complex can be found in [Reshetnyak, 2007; 2008; Reshetnyak and Hejda, 2008]. The calculations are carried out on the 64^3 grids.

3. RESULTS OF SIMULATION

We consider two modes of convection (and dynamo):

R1: Mode with rotation, $\mathrm{Ra} = 4 \times 10^2$, $\mathrm{Pr} = 1$,

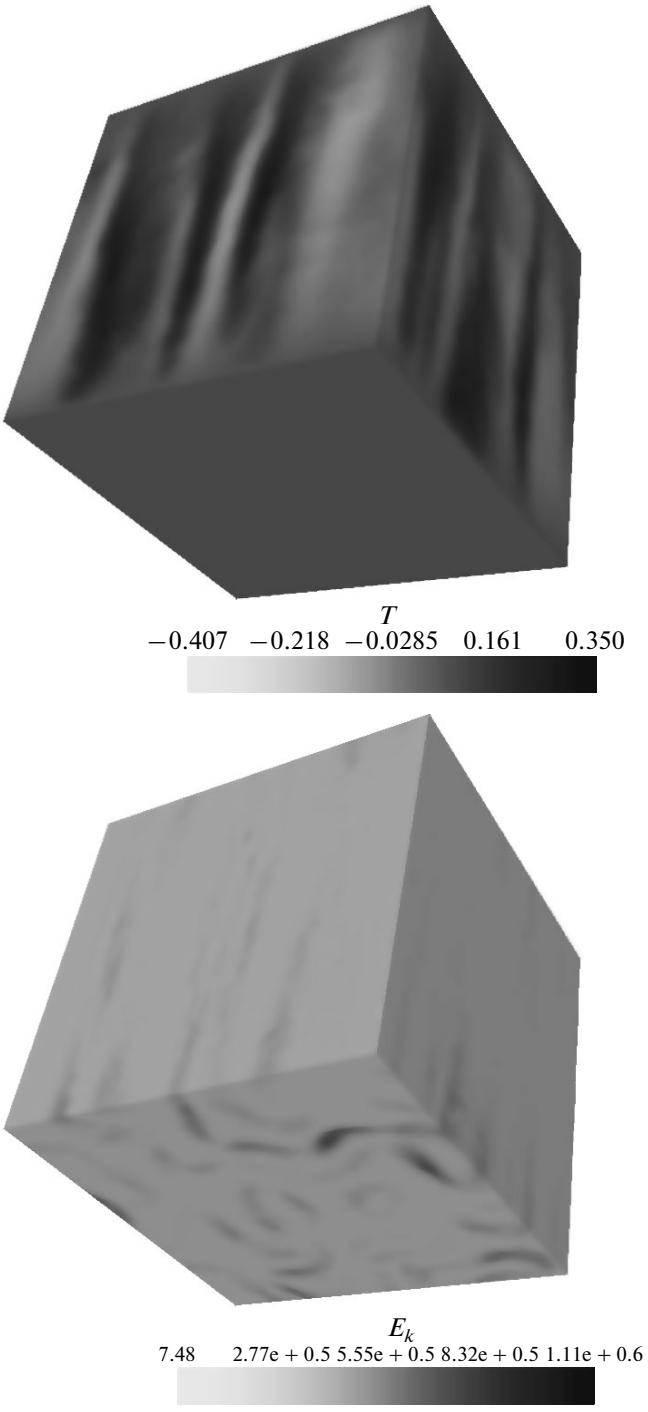

Fig. 1. The distribution of the disturbance of temperature T and kinetic energy E_K for R2 mode.

$$E = 2 \times 10^{-5}, q = 10.$$

R2: Mode with rotation, $\mathrm{Ra} = 1 \times 10^3$, $\mathrm{Pr} = 1$,

$$E = 2 \times 10^{-5}, q = 3.$$

Both modes correspond to the geostrophic (magnetostrophic) balance of forces. The typical distribution of the fluctuations in temperature T and kinetic energy $E_\mathrm{K} = \frac{V^2}{2}$ (mode R2) are presented in Fig. 1. A

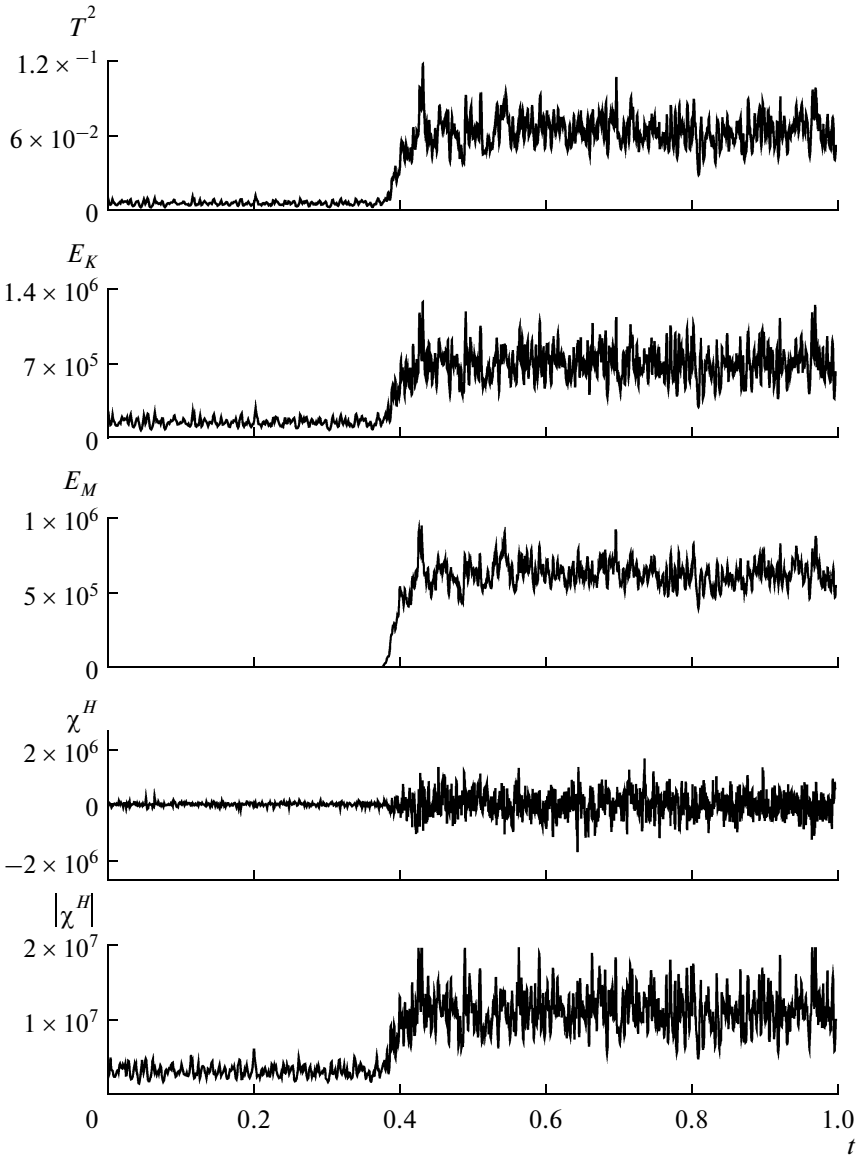

Fig. 2. The evolution of the volume-average fluctuations of the squared temperature T^2, the kinetic and magnetic energy E_K, E_M, and the hydrodynamic helicity χ^H and $|\chi^H|$ for the R1 mode.

characteristic feature of these distributions is the existence of structures elongated along the rotational axis z, which correspond to the cyclonic and anticyclonic vortices. The diameter of the vortices is determined by the Ekman number $d_c \sim \mathrm{LE}^{1/3}$ [Busse, 1970].

Now, we consider the evolutionary characteristics of the system in greater detail. For both modes Rl and R2, the problem of heat convection (1) without the magnetic field was calculated. Further, after the adjustment of the quasiperiodic solution at the time moment $t = 0.35$, the magnetic field $\mathbf{B}_0$ with small amplitude was introduced, which led to an exponential increase in the magnetic energy $E_M = \dfrac{B^2}{2\mathrm{Ro}}$ (the kinematic dynamo mode) and the subsequent attainment of the quasistationary state, see Figs. 2, 3. In both the considered cases, this transition is accompanied by the increase in the fluctuations of the squared temperature T^2. At the same time, the behavior of the kinetic energy E_K is different: in the first case, an increase in the magnetic field leads to the increase in the kinetic energy, whereas in the second case it results in the decrease of the kinetic energy. In the R1 mode, the magnetic field contributes to the disturbance of the geostrophic flow, to the formation of its 3D structure and, as a consequence, to an increase in the efficiency of the magnetic field generation. The sum $E_K + E_M$ has increased. The R2 mode corresponds now to a more disturbed state of convection relative to the geostrophic state; and a part of the kinetic energy is simply

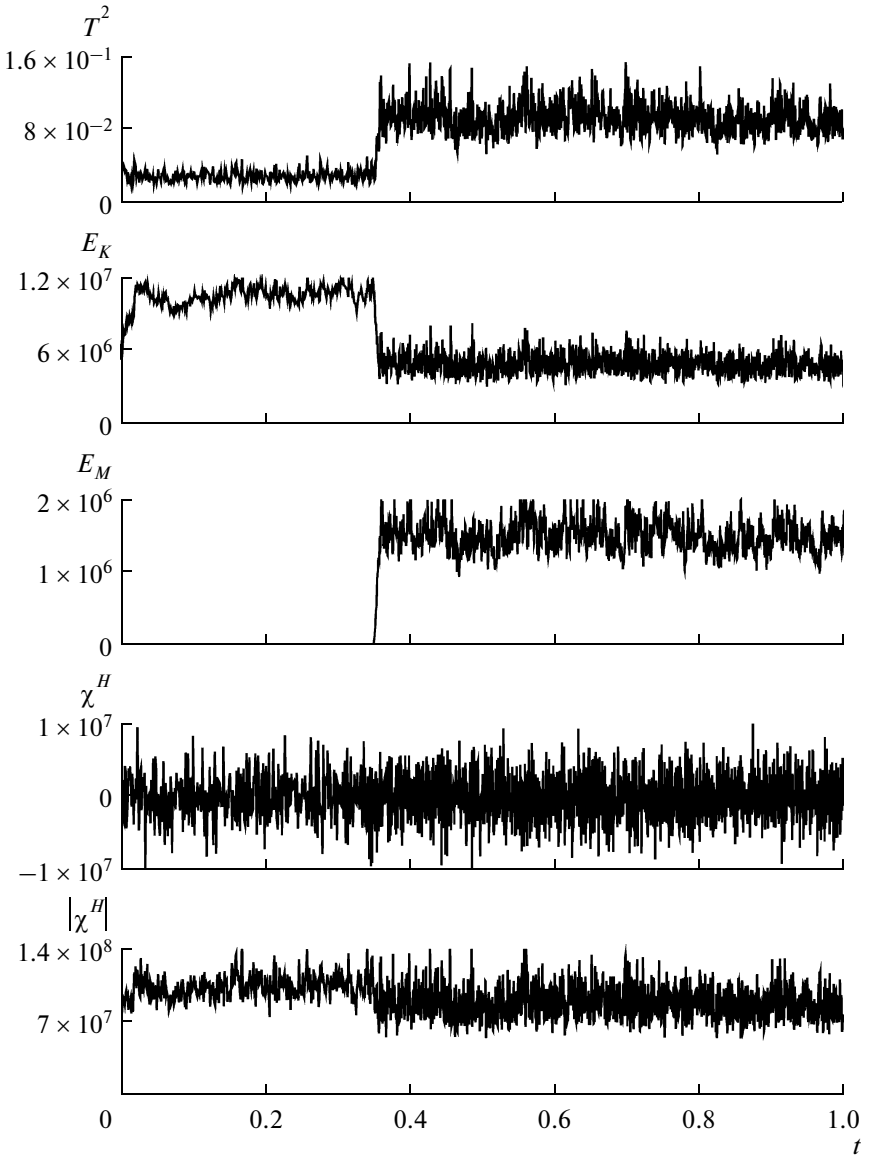

Fig. 3. The evolution of the volume-average fluctuations of the squared temperature T^2, the kinetic and magnetic energy E_K, E_M, and the hydrodynamic helicity χ^H and $|\chi^H|$ for the R2 mode.

consumed on an increase in the magnetic energy. The sum $E_K + E_M$ has slightly decreased. For the developed convection, the R2 mode is more typical. It is worth noting that in the first case, an increase in the amplitude of T^2 resulted in an increase of the work of the Archimedean forces $\mathbf{F_a} = \mathrm{Ra}\mathbf{T}1_z$ (the work is $W_a = \mathrm{Ra}TV_z$), and in the second case an increase in the fluctuations of T occurred against a background reduction in the efficiency of $\mathbf{F_a}$ due to the chaotization of the convection by the magnetic field and resulted in the weakening of the correlation between the fields T and $\mathbf{V}$.

The behavior of the hydrodynamic helicity $\chi^H = \mathbf{V} \cdot \mathrm{rot}\mathbf{V}$, is generally similar to the behavior of the kinetic energy. A characteristic feature is an increase in the variance χ^H with the appearance of the magnetic field.

3.1. The Spectral Properties

Now, we consider the spectra of the fields. The maximum of the spectrum of kinetic energy for R1 (Fig. 4a) corresponds to the cyclonic-scale structures ($k_c = 1/d_c$). In passing from the convection to the dynamo mode, a portion of energy is transferred from the smaller to larger scales, and the maximum becomes less distinct. The total increase of kinetic energy occurs.

An increase in the magnetic field in passing from the kinematic dynamo mode to the quasi-stationary state is accompanied by an increase in the magnetic energy at larger scales (Fig. 4b). The maximum saturation is achieved first by the modes with $k \sim 10$; further, the saturation of the spectrum for smaller k occurs. A similar pattern is also observed for R2 (Fig. 4d). An exception is the

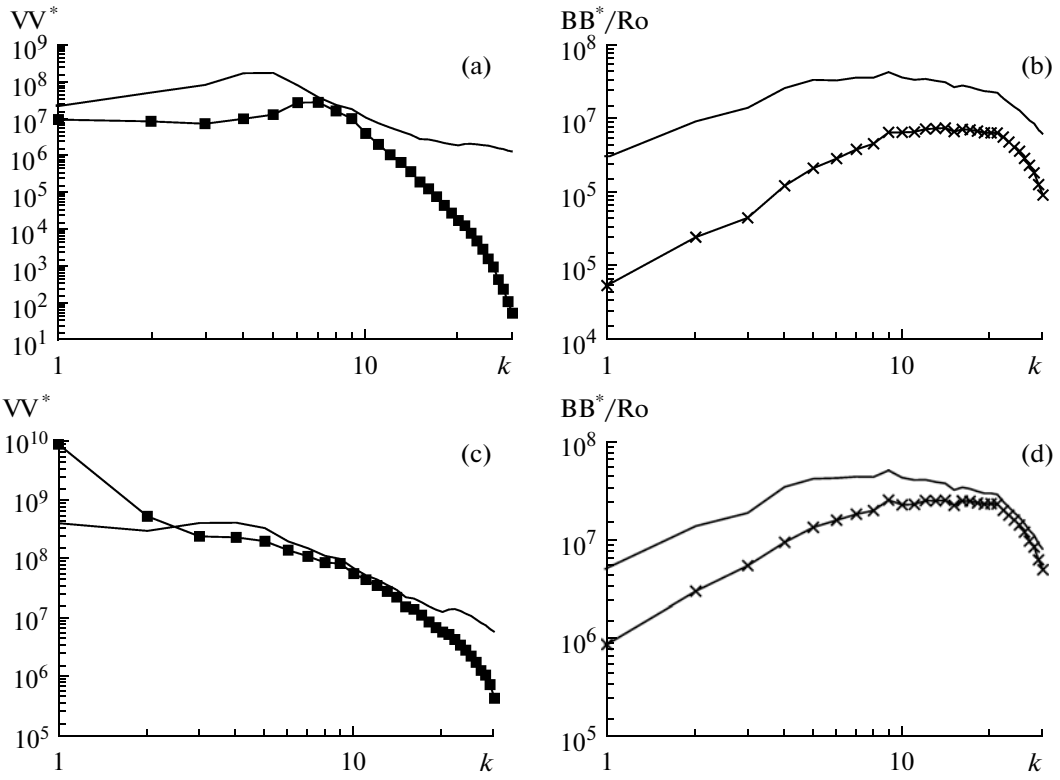

Fig. 4. Spectra of kinetic and magnetic energy for the R1 mode (a, b) and the R2 mode (c, d). The solid line corresponds to the steady dynamo mode; the squares correspond to the convection without the magnetic field; and the crosses correspond to the kinematic dynamo mode.

behavior of the kinetic energy at large scales (Fig. 4c): the magnetic field leads to the destruction of horizontal rolls, which results in the vanishing of the maximum of kinetic energy for $k = 1$.

A nonuniform growth of the magnetic field for different k is of significant importance for the process of stabilization. An increase in the magnetic field in the conditions of kinematic dynamo occurs on the convective periods $\tau_k \sim (kV_k)^{-1}$ that obviously decrease with increasing k. For nonrotating turbulence, according to the Kazantsev model [Kazantsev, 1967], the spectrum of the growing magnetic field in the kinematic dynamo mode is $E_M \sim k^{3/2}$, and, correspondingly, the maximum falls in the range near the dissipative scale. According to the Kazantsev model, the appearance of the magnetic flux ropes with a typical size of $\sim R_m^{1/2}$, is possible, which results in the magnetic field becoming intermittent; and the volume-average magnetic energy turns out to be less than the volume-average kinetic energy [Subramanian, 1998]. In our case, the existence of the maxima in the spectra of E_K at $k = k_c$ turns out to be of crucial importance, and the modes which first attain the saturation are those with $k \sim k_c$.

The observed redistribution of the magnetic field over the scales is closely connected with the conservation over the volume of magnetic helicity $\chi^M = \mathbf{A} \cdot \mathbf{B}$ at $R_m \longrightarrow \infty$ [Berger, 1984], where $\mathbf{A}$ is the vector potential of the magnetic field: $\mathbf{B} = \mathrm{curl}\mathbf{A}$. The large values of R_m are typical for the majority of astrophysical objects that possess their own magnetic fields. The value of χ^M characterizes the linkage between the magnetic field lines [Moffat, 1978]; and it can change the sign. From the induction equation one may derive the equation for the average values:

$$\frac{D}{Dt}\overline{\mathbf{AB}} = -R_m\overline{\mathbf{JB}} + \Pi, \qquad (2)$$

where $\mathbf{J} = \mathrm{curl}\mathbf{B}$ is the current, and Π is the flux of χ^M through the boundary of the domain (see details in [Subramanian, 1998]). For fully periodical boundary conditions, or superconducting boundaries, $\Pi = 0$. The quantity $\chi^J = \mathbf{J} \cdot \mathbf{B}$ is called the current helicity.

Then, for the time $t \sim R_m \gg 1$ after the equilibration, $\frac{D}{Dt} = 0$, and have:

$$\bar{\mathbf{J}} \cdot \bar{\mathbf{B}} = -\overline{\mathbf{jb}}, \ \bar{\mathbf{A}} \cdot \bar{\mathbf{B}} = -\overline{\mathbf{ab}}, \qquad (3)$$

where the fields are represented as a sum of the mean value and the fluctuation component: $F = \bar{F} + f$. In other words, after the termination of the exponential increase in the magnetic field, the redistribution of the

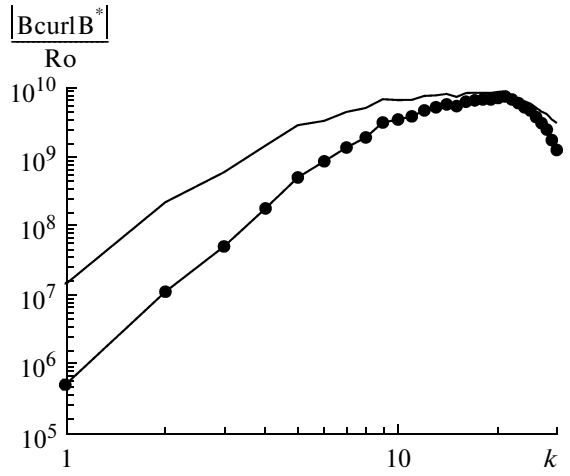

Fig. 5. Spectra of current helicity for the R1 mode. The solid line corresponds to the steady dynamo mode; the circles correspond to the kinematic dynamo mode.

magnetic field over the scales is possible such that it provides the zero total current helicity.

The use of the pseudovacuum boundary conditions with the nonzero flux of the helicity at the boundaries $\Pi \neq 0$ makes it possible to increase the energy of the large-scale magnetic field B_0 [Brandenburg and Sandin, 2004]. At the same time, for the periodic boundary conditions, a catastrophic suppression of the generation of the magnetic field is observed on the large scales $B_0^2 \sim \mathrm{R}_\mathrm{m}^{-1} b_{Eq}^2$, where $b_{Eq}^2 \sim \nu^2$ is the energy of small-scale fields [Vainshtein and Cattaneo, 1992]. The latter phenomenon is easily observed for the R1 and R2 modes: the magnetic and kinetic energies are approximately of the same order of magnitude, while the magnetic helicity on the large scales substantially increases when the quasistationary mode is attained (see Fig. 5).

It is interesting that in the dynamo theory of average fields [Pouquet et al., 1976; Zeldovich et al., 1983], there is a relation between the hydrodynamic and the current helicities, and between the hydrodynamic α^H and the magnetic α^M effects:

$$\alpha^H = -\tau\overline{\mathbf{v}\cdot\omega}/3,\ \alpha^M = \tau\overline{\mathbf{jb}}/3, \quad (4)$$

where $\omega = \mathrm{curl}\mathbf{v}$ is the vorticity, and τ is the correlation time. Then, the total α effect is

$$\alpha = \alpha^H + \alpha^M. \quad (5)$$

If the signs of the helicities coincide, then the total α effect decreases ($\alpha^M \longrightarrow -\alpha^H$) and the magnetic field ceases to grow. This can be clearly seen in Fig. 6 where, at $z < 0.5$, the sign of helicities is positive, and at $z > 0.5$ it is negative. The fluctuations in the current helicity are associated with the fact that the magnetic field is more indented than the velocity field. A similar vertical distribution is also observed in the magnetic helicity χ^M and in the so-called cross-helicity $\chi^C = \mathbf{VB}$ (see Fig. 7).

3.2. Energy Fluxes in the Wave Space

The spectral redistribution of energy is related to a change in the energy fluxes in the wave space. In spite of the statistical stationarity of the dynamo processes considered, these processes are dissipative (i.e., irreversible) and, in the strict sense, they are nonequilibrium processes [Rose and Sulem, 1978]. For the simplest cases (for example, in the 3D Kolmogorov turbulence), the latter is expressed in the directed energy fluxes in the wave space with the transfer of energy from the generation scales (inertial range) to the dissipation scales [Frisch, 1995].

Further, we repeat the results presented in [Reshetnyak and Hejda, 2008] and discuss the difference between the kinematic dynamo mode and the nonlinear mode. Let us consider the energy fluxes in the wave

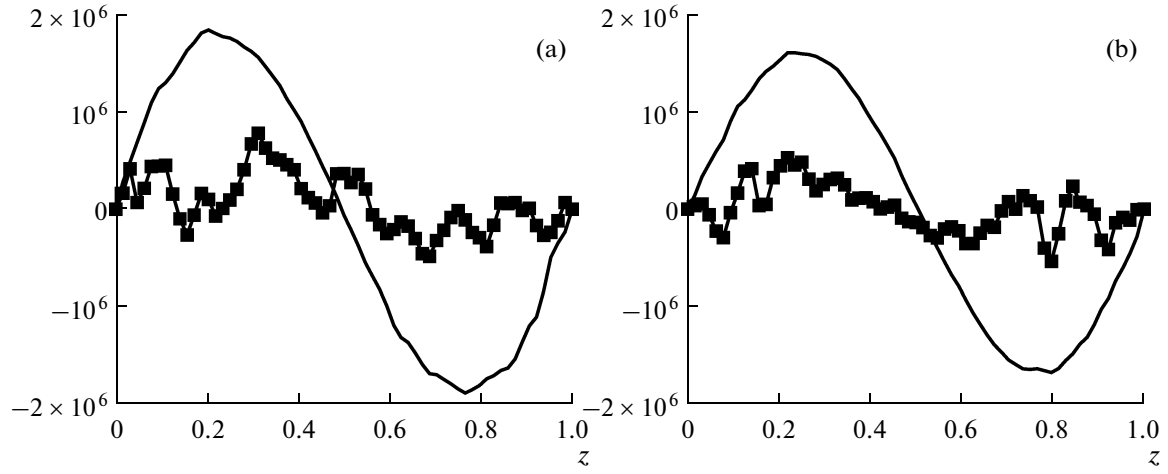

Fig. 6. Profiles of the hydrodynamic χ^H (the solid line) and current χ^J (the squares) helicities for (a) the R1 and (b) R2 modes, respectively.

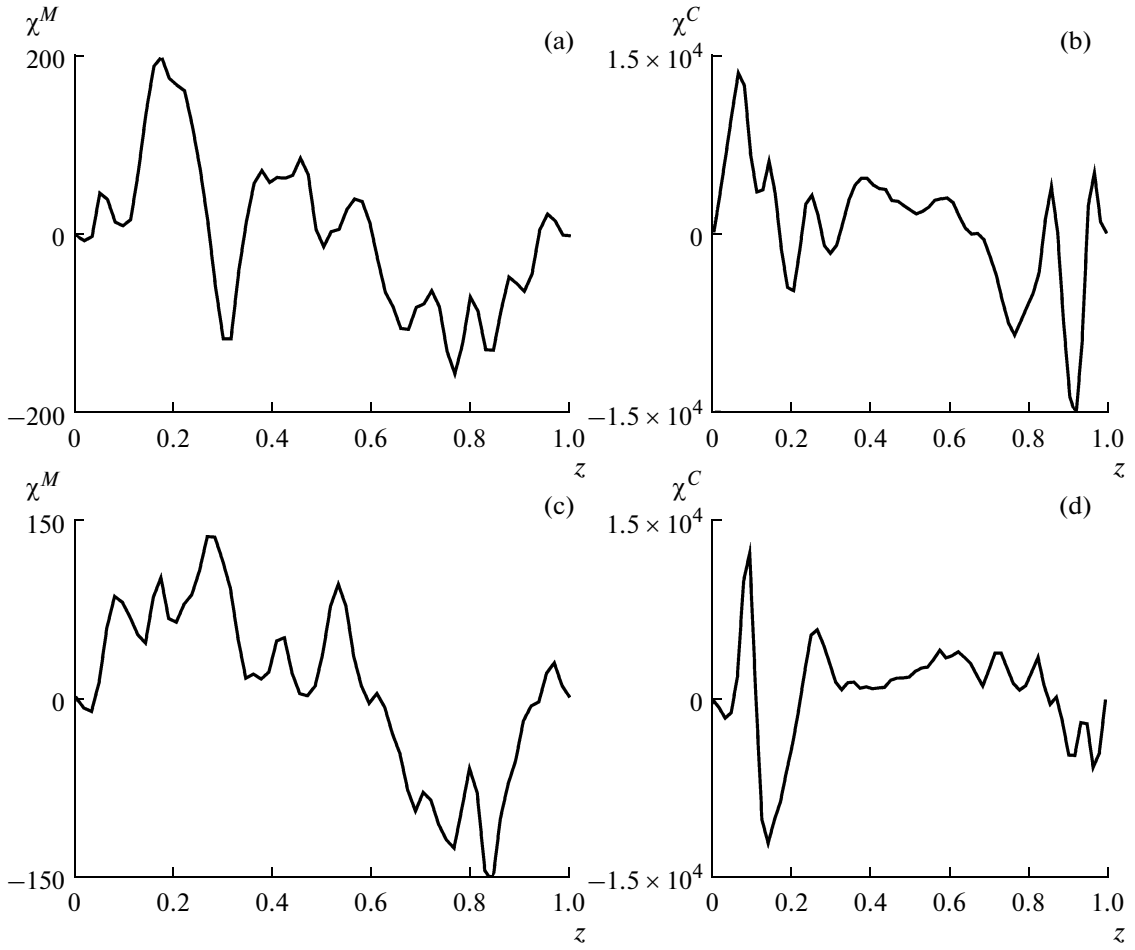

Fig. 7. Profiles of the magnetic χ^H and the cross- χ^C helicities for the R1 (a, b) and R2 (c, d) modes.

space $T(k)$ through the wave number k and introduce the following designations for the kinetic energy flux $T(k)$, $\int_0^\infty T_K(k)dk = 0$ and for the magnetic energy flux $T_M(k)$.

By virtue of the relationship of the $\text{curl}(\mathbf{V} \times \mathrm{B}) = -(\mathbf{V} \cdot \nabla)\mathbf{B} + (\mathbf{B} \cdot \nabla)\mathbf{V}$, the flux $T_M(k)$ can be represented as a sum of two components, the advective and the generation ones: $T_M = T_N - T_L$, $\int_0^\infty T_N(k)dk = 0$. The latter is assumed to be equal to the work of the Lorentz forces taken with the opposite sign.

The fluxes of kinetic energy T_K are depicted in Figs. 8a and 9a. For $k \sim k_c$, the inverse cascade of kinetic energy is observed: the cyclones are the energy sources; they transfer the energy both on the larger scales ($k < k_c$, $T_K > 0$) and on the smaller scales ($k > k_c$, $T_K > 0$) (the direct cascade), where it dissipates. The magnetic field causes a certain diffusion of the maxima and a small shift of T_K toward the long-wave region.

In contrast to T_K, T_M includes not only the transfer term, but also the generation term. It turns out that the integral of T_M over the entire wave space is positive. Furthermore, T_M is positive everywhere (see Figs. 8b and 9b); i.e., the magnetic field is generated by the small-scale flows. The position of the maximum in T_M is close to the position of the maximum in the spectrum of E_M. The shape of T_M remains unchanged when passing from the weak magnetic field mode to the nonlinear mode. Let us dwell on what is the source of the magnetic energy: whether this is connected with the energy transfer across the spectrum, or with the processes of generation.

The fluxes $-T_L$ associated with the generation term are displayed in Figs. 8c and 9c. The maximum in $-T_L$ is close to the minimum in T_K (R1), which reflects the fact of the conversion of the kinetic energy of a cyclone into the magnetic field energy. The inverse energy cascade $-T_L > 0$ is observed everywhere except for a small high-frequency domain. It is worth noting that the amplitudes of the maxima in $-T_L$ and T_M are essentially different. This is due to the fact that the terms $-T_L$ and T_N are phase-opposite (see Figs. 8d and 9d). The latter means that the advective term $T_N < 0$ transfers the entire obtained magnetic energy into the dissipation domain (large k).

For the R1 mode, the passage to the nonlinear conditions barely changes the configuration of the flows and

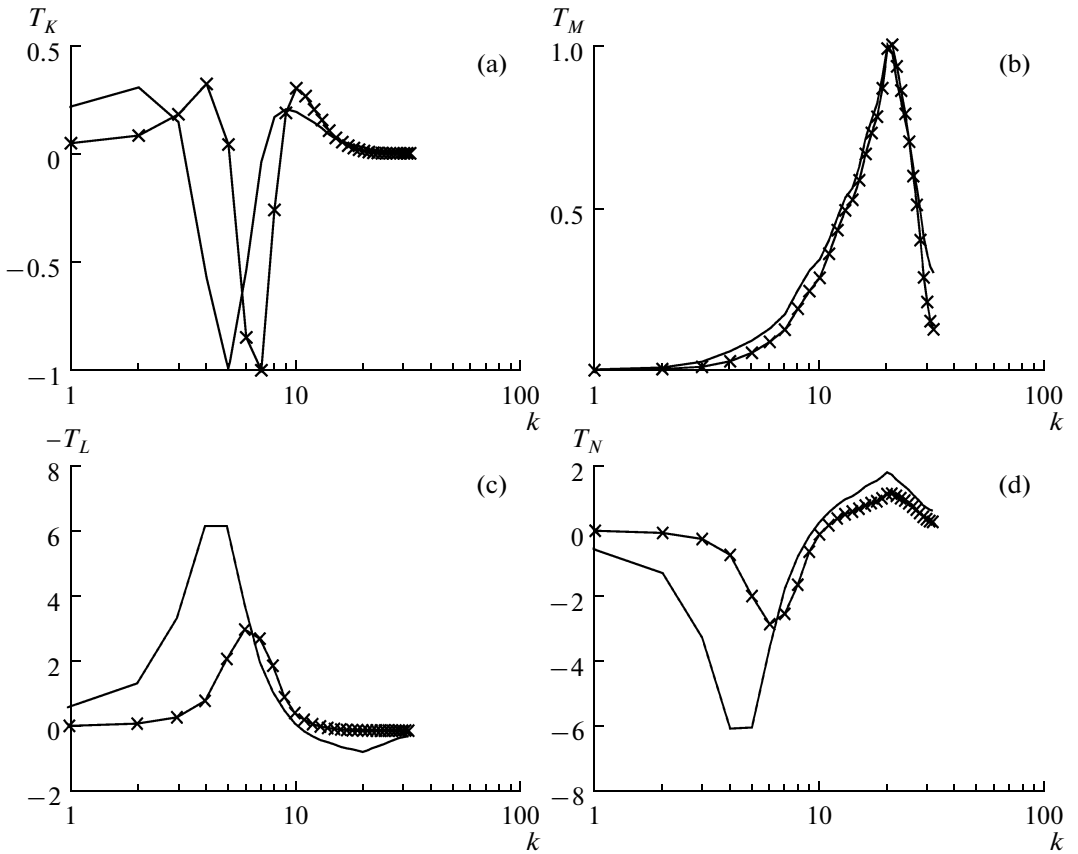

Fig. 8. Fluxes of the kinetic T_K and magnetic T_M energies in the wave space, the work of the Lorentz force T_L and of the convective term in the equation of induction T_N for the R1 mode. The solid line corresponds to the steady dynamo mode; the crosses correspond to the kinematic dynamo mode.

enhances the amplitudes of $-T_L$ and T_N; i.e., the synchronization of two fluxes increases.This effect is also observed for the R2 mode, but in this case the curves also change their shapes. After the passage to the nonlinear conditions, a pronounced extremum appears at $k \sim k_c$, which appears to be associated with the fact that for the R2 mode, the ratio E_M/E_K is smaller, and the influence of the shape of the kinetic energy spectrum on the behavior of the curves is stronger.

4. Equilization of the Fields

Until now, when examining the distribution of helicities over z, we have disregarded the importance of the correlation between the fields **V** and **B**. In the work [Cattaneo and Tobias, 2009], the following numerical experiment was carried out: after solving the dynamo problem and attaining the quasistationary conditions, the authors added to the system one additional equation of induction with the new, artificial magnetic field $\hat{\mathbf{B}}$. The difference of this magnetic field from the initial one was that it did not affect the velocity field. Further, after taking the slightly disturbed values of the current magnetic field $\hat{\mathbf{B}}$ as the initial conditions for the new field **B**, the authors continued the calculations and used the velocity **V** from the initial dynamo system. It turned out that the magnetic energy of the new magnetic field exponentially increases despite the fact that the system has already passed into saturation mode. In the experiment, the authors used the cascade models and a 3D code with the periodic boundary conditions with a constrained force. An exponential increase in the field $\hat{\mathbf{B}}$ was observed in both cases. Now, we consider the situation in more detail and include, in addition, also the heat transfer equation:

$$\begin{aligned}
\frac{\partial \mathbf{B}}{\partial t} &= \mathrm{curl}(\mathbf{V}\times\mathbf{B}) + \mathrm{q}^{-1}\Delta\mathbf{B}\\
\mathrm{EPr}^{-1}\left[\frac{\partial \mathbf{V}}{\partial t} - \mathbf{V}\times(\nabla\times\mathbf{V})\right] &= \mathrm{curl}\mathbf{B}\times\mathbf{B}\\
-\nabla P - 1_z\times\mathbf{V} + \mathrm{Ra}T1_z + \mathrm{E}\Delta\mathrm{V}&\\
\frac{\partial T}{\partial t} + (\mathrm{V}\cdot\nabla)(T+T_0) &= \Delta T\\
\frac{\partial \hat{\mathbf{B}}}{\partial t} &= \mathrm{curl}(\mathrm{V}\times\hat{\mathbf{B}}) + \mathrm{q}^{-1}\Delta\hat{\mathbf{B}}.
\end{aligned} \qquad (6)$$

The behavior of the magnetic energy for the fields **B** and $\hat{\mathbf{B}}$ is presented in Fig. 10. In spite of the use of the same velocity for the magnetic field in both equations of induction, the behavior of energy is different: for the

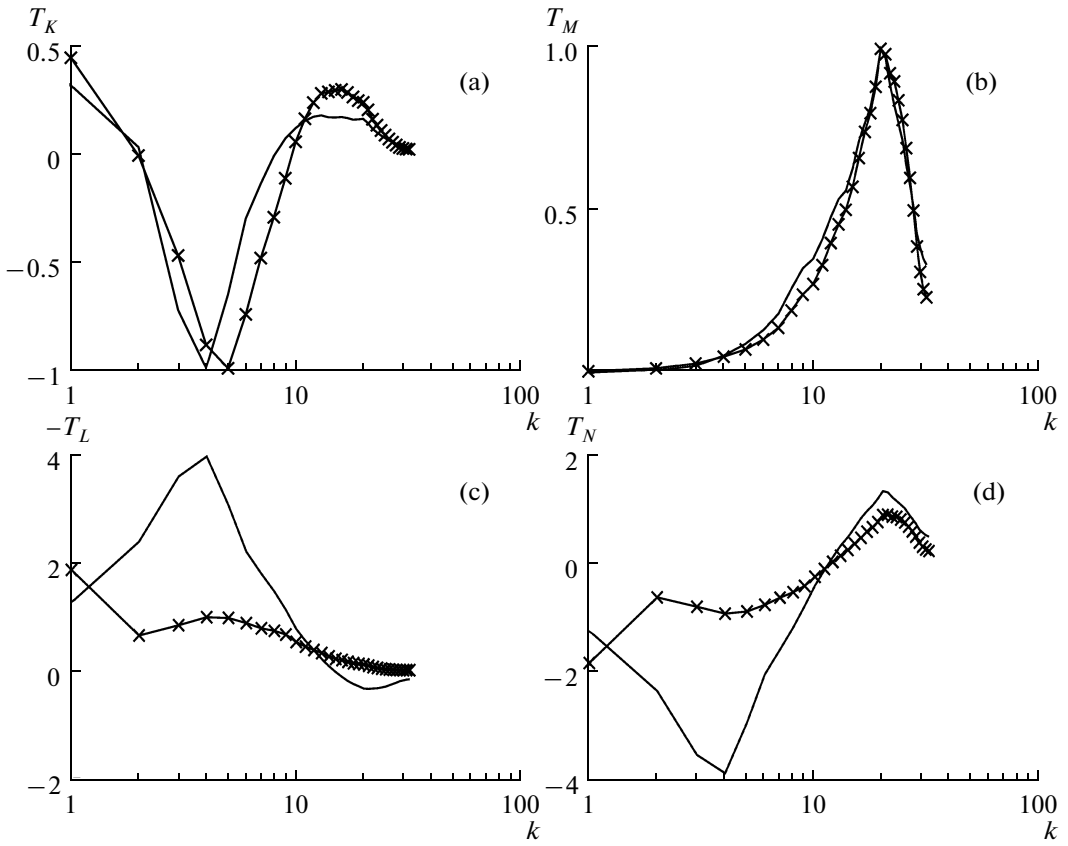

Fig. 9. Fluxes of the kinetic T_K and magnetic T_M energies in the wave space, the work of the Lorentz force T_L and of the convective term in the equation of induction T_N for the R2 mode. The solid line corresponds to the steady dynamo mode; the crosses correspond to the kinematic dynamo mode.

field **B** it remains at a certain quasistationary level, while for the field $\hat{\mathbf{B}}$ it exponentially increases with time. We assume that the time synchronization of the field of velocity and the magnetic field is extremely important. This synchronization is deliberately less for the field $\hat{\mathbf{B}}$, since there is no Lorentz force for this field. In order to demonstrate this, we consider the evolution of the spatiotemporal correlation of the fields Corr(V, B), Corr(V, $\hat{B}$), calculated over the half volume $z \le 0.5$ (see Figs. 11 and 12). One can clearly see that for both the R1 and R2 modes, the correlation for $\hat{\mathbf{B}}$ is smaller than for **B**. The correlation does not

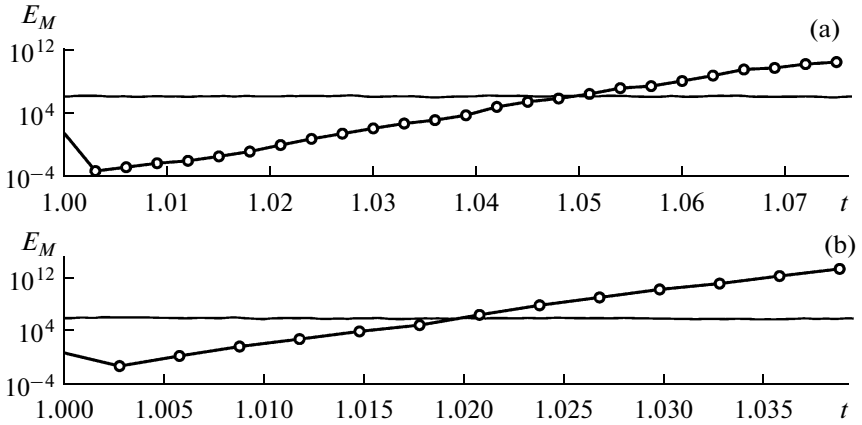

Fig. 10. The evolution of the magnetic energy $B^2/2$ (the solid line) and the field energy $\Psi^2/2$ (circles) for (a) the R1 and (b) R2 modes.

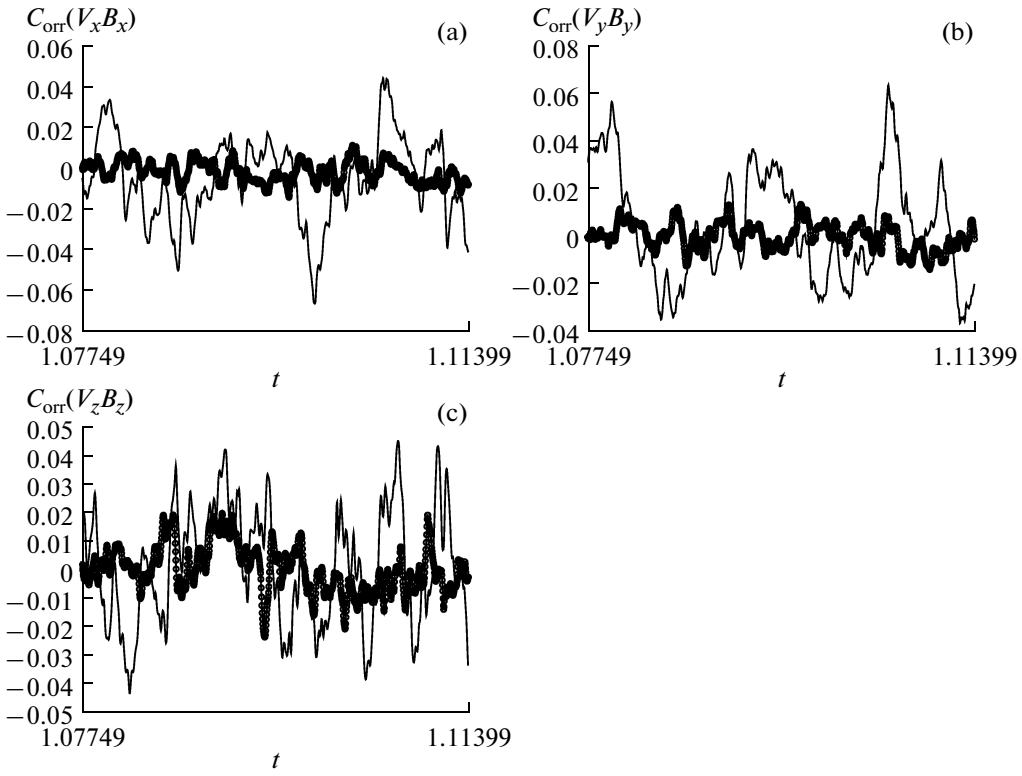

Fig. 11. The evolution of the spatial autocorrelation functions for the R1 mode.

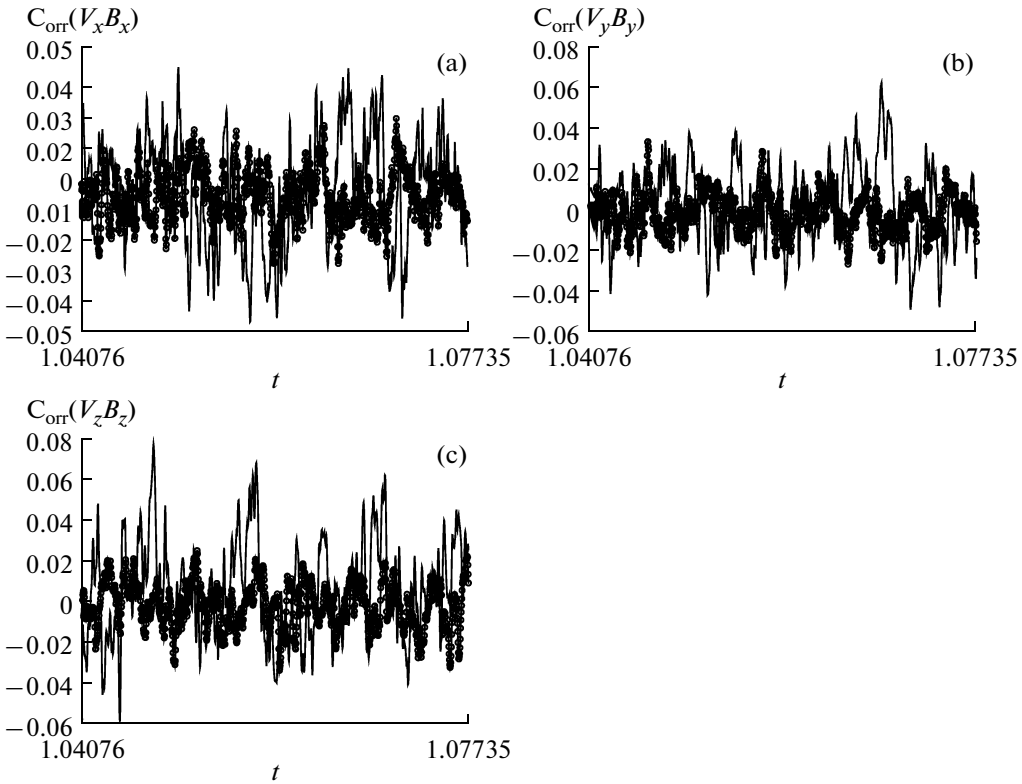

Fig. 12. The evolution of the spatial autocorrelation functions for the R2 mode.

exceed several percent for either of the magnetic fields due the large contribution of the small-scale component. The componentwise decrease of the correlations is simply the reduction in the equalization (codirectivity) of the velocity field and the magnetic field. The actual magnetic field **B** is equalized with the field **V** to a greater degree, than field $\hat{\mathbf{B}}$.

5. DISCUSSION AND CONCLUSIONS

The transition from the exponential growth of the magnetic field to the nonlinear dynamo mode in the cyclonic flows is accompanied by a number of processes, which are listed below. Upon this transition, a change in the kinetic energy of the system is not of fundamental importance: E_K can either increase or decrease. The effect of the magnetic field on the flow patterns is more essential.

Assume that the generation magnetic field **B** begins in the conditions of steady-state heat convection with nonzero helicity $\chi^H(z)$. The eigenfunction of **B** increases up to the level when the maximum of the spectrum, which falls on large k reaches a certain value, which is comparable in amplitude with the value of the kinetic energy on this scale. Further, the small-scale magnetic field **b** ceases growing. The process is accompanied by the appearance of the magnetic α^M effect, which leads to the decrease of the total α effect (5). According to (3), the equilibration requires an increase of the large-scale field, which really occurs on the convective periods corresponding to the large scales. The influence of the Lorentz force that leads to the correlation of the fields **V** and **B** and to their equalization relative to each other, is of fundamental importance. The transient processes during the stabilization of a large-scale magnetic field are undoubtedly important for understanding the mechanisms of the processes of the geomagnetic reversals and the excursions of the geomagnetic field.

REFERENCES

1. M. A. Berger, "Rigorous New Limits on Magnetic Helicity Dissipation in the Solar Corona," Geophys. Astrophys. Fluid Dynamics **30** 79–104 (1984).
2. A. Brandenburg and C. Sandin, "Catastrophic Alpha Quenching Alleviated by Helicity Flux and Shear," Astron. Astrophys. **427**, 13–21 (2004).
3. A. Brandenburg and K. Subramanian, "Astrophysical Magnetic Fields and Nonlinear Dynamo Theory," Phys. Rep. **417**, 1–209 (2005).
4. F. H. Busse, "Thermal Instabilities in Rapidly Rotating Systems," J. Fluid Mech. **44**, 441–460 (1970).
5. F. Cattaneo and S. M. Tobias, "Dynamo Properties of the Turbulent Velocity Field of a Saturated Dynamo," J. Fluid Mech. **621**, 205–214 (2009).
6. S. Chandrasekhar, *Hydrodynamics and Hydromagnetic Stability* (Dover Publications Inc., New York, 1981), pp. 1–654.
7. U. Frisch, *Turbulence: The Legacy of A. N. Kolmogorov* (Cambridge University Press, Cambridge, 1995), pp. 1–296.
8. C. A. Jones, "Convection-Driven Geodynamo Models," Phil. Trans. R. Soc. London **A358**, 873–897 (2000).
9. A. P. Kazantsev, "About Magnetic Field Amplification by the Conducting Liquid," Soviet Physics—JETP **53**, 1806–1813 (1967).
10. F. Krause and K.-H. Radler, *Mean Field Magnetohydrodynamics and Dynamo Theory* (Akademie-Verlag, Berlin, 1980), pp. 1–271.
11. H. K. Moffatt, *Magnetic Field Generation in Electrically Conducting Fluids* (Cambridge University Press, Cambridge, 1978), pp. 1–343.
12. A. Pouquet, U. Frisch, and J. Leorat, "Strong MHD Helical Turbulence and the Nonlinear Dynamo Effect," J. FIuid Mech. **77**, 321–354 (1976).
13. M. Yu. Reshetnyak, "Thermal Convection and the Dynamo during Rapid Rotation," Fiz. Zemli, No. 8, 23–32 (2007) [Izv. Phys. Solid Earth **43** (8), 642–652 (2007)].
14. M. Yu. Reshetnyak, "Certain Spectral Properties of Cyclonic Turbulence in the Earth's Liquid Core," Geomagn. Aeron. **48** (3), 416–423 (2008) [Geomagnetism and Aeronomy **48** (3), 400–407 (2008)].
15. M. Reshetnyak and P. Hejda, "Direct and Inverse Cascades in the Geodynamo," Nonlin. Proc. Geophys., **15**, 873–880 (2008).
16. H. A. Rose and P. I. Sulem, "Fully Developed Turbulence and Statistical Mechanics," J. Physique **39**, 441–484 (1978).
17. K. Subramanian, "Can the Turbulent Galactic Dynamo Generate Large-Scale Magnetic Fields?" Mon. Not. R. Astron. Soc., **294**, 718–728 (1998).
18. S. T. Vainshtein and F. Cattaneo, "Nonlinear Restrictions on Dynamo Action," Astrophys. J. **393**, 165–171 (1992).
19. Ya. B. Zeldovich, A. A. Ruzmaikin, and D. D. Sokoloff, *Magnetic Fields in Astrophysics* (Gordon and Breach, New York, 1983), pp. 1–436.